Hindawi
Adsorption Science & Technology
Volume 2023, Article ID 8581697, 13 pages
https://doi.org/10.1155/2023/8581697

Research Article

Optimization of the Fabrication of Sustainable Ceramsite Adsorbent from Coal Fly Ash/Waterworks Sludge/Waste Glass for Decolorization of Malachite Green

Weicheng Fang, Xingxing Cheng, Chang-Jung Sun, Hongfei Xiao, and Jing Wang

Department of Environmental Science and Engineering, City College of Dongguan University of Technology, Dongguan 523419, China

Correspondence should be addressed to Xingxing Cheng; 1447839402@qq.com

Received 25 October 2022; Revised 7 December 2022; Accepted 31 December 2022; Published 3 February 2023

Academic Editor: Muhammad Raziq Rahimi Kooh

As a traditional dye, malachite green (MG) poses a threat to our environment and health. To decolorize MG, a composite ceramsite adsorbent composed of coal fly ash (CFA), sewage treatment sludge (STS), and waste glass (WG) with a quality ratio of 3 : 3 : 4, respectively, was prepared. The optimal preparation parameters were determined as follows: preheating temperature = 600 ∘ C, sintering temperature = 1157 ∘ C, and sintering time = 17 min. Under optimal conditions, scanning electron microscopy (SEM) images show that the X-Com-ceramsite sample exhibits rough features and a porous structure. The obtained X-Com-ceramsite has a good MG decolorization effect (92% decolorization rate with an initial MG concentration of 56.876 mg/L). The q_{max} value of MG can reach up to 37.6 mg/g. The retention degree of MG in the X-Com-ceramsite with a relatively higher pH is stronger, and the adsorption process is spontaneous and endothermic. Synchronous fluorescence, two-dimensional correlation spectroscopy (2D-COS), and Fourier transform infrared spectroscopy (FT-IR) proved that the sensitivity of the C-O/C-O-O functional groups of the carbohydrates on the surface of the X-Com-ceramsite has a higher binding affinity toward MG as the initial concentration of MG changes.

1. Introduction

Malachite green (MG), a common synthetic triphenylmethane, was widely used in the textile industry and fishery [1]. Nowadays, over 10000 types of dyes are being manufactured, and the annual worldwide dye production is more than 700000 tons [2]. Unfortunately, once released into the surface water environment, MG will prevent sunlight from penetrating the bulk volume of the affected water systems and therefore reduces the dissolved oxygen (DO) level in the water [3]. It is thus crucial to remove MG residues from industrial wastewater. Adsorption method attracts increasing research attention as it is straightforward and reliable, exhibiting design flexibility and renewability [4]. Thus, one of the most critical scientific issues is the synthesis of cheap, accessible, and effective adsorbents.

Ceramsite is a lightweight artificial aggregate initially applied in building materials to replace coarse aggregate gravel and pebbles mixed in concrete. With the expansion of research on the properties of different ceramsite, the application of ceramsite has gradually expanded, mainly in the fields of environmental protection [5], construction [6], sound absorption [7], horticulture [8], and others. In recent years, due to its high strength, low density, rough and porous surface, large specific surface area, and other great characteristics [9], ceramsite has been widely used in wastewater treatment [5]. For example, Fu and Dai [10] prepared porous ceramsite (TL530) with paper-making sludge, showing a high removal efficiency of Cu^{2+} (98.13%, the initial concentration was 100 mg/L). Zhu et al. [11] used sludge and fly ash as raw materials to prepare composite ceramsite, and the maximum adsorption amount of total P reached

1.199 mg/g. In particular, Wu et al. [12] reported that the maximum adsorption capacity of arsenic by ceramsite as the filler of constructed wetland reached 25.39 mg/kg, which is much higher than that of zeolite (11.96 mg/kg) and gravel as a filler (7.04 mg/kg). These results indicated that ceramsite is an efficient sorbent with high application potential. However, traditional raw materials used for ceramsite preparation are nonrenewable, so they were officially prohibited or restricted in China [13]. Therefore, using other accessible materials to replace clay, shale, and other nonrenewable resources to produce ceramsite has become popular.

Sewage treatment sludge (STS) is the by-product produced in domestic sewage treatment and is widely considered a type of industrial waste [14]. According to the data released by the Ministry of Environmental Protection, PRC, in 2015 [15], the annual production of municipal STS exceeds 40 million tons. It contains many toxic substances, such as heavy metals [16], pathogenic bacteria [17], and organic pollutants, and it is estimated to exceed 60 million tons by 2020 [18]. Fly ash is a solid particulate matter from the electric power industry [19]. It was reported in 2020 that the annual output of fly ash in China's industrial enterprises in 2019 was about 5.4×10^8 t, of which about 25% was not utilized [20]. Accumulated fly ash generates dust and pollutes the air [21]. Further, it leaches sediments in the water. Therefore, air and land waste pollution caused by a large amount of fly ash stacking should be considered.

The chemical composition of raw materials is the main factor affecting the swelling properties of ceramsite. It was reported that the physical and chemical properties of sludge are similar to the composition of traditional raw materials used to prepare ceramsite [22]. In addition, organic matter in sludge produces volatile compounds and reduces the carbon content during the sintering process, and its inorganic components generate new crystal structures at high temperatures. Taking advantage of these two characteristics of the sludge, it can be mixed with other materials to prepare sludge ceramsite that can adsorb pollutants under suitable operating conditions. Wan et al. [23] used sludge, fly ash, clay, and glass powder as raw materials to conduct single-factor experiments to investigate the effects of various properties of ceramsite prepared at different raw material ratios and firing processes. Cheng et al. [24] used urban sludge and incinerated ash as raw materials to analyze the influence of process conditions and the material ratio on water absorption and the density of ceramsite by single-factor experiments. Rong et al. [25] reported that the sintering and preheating temperatures significantly influence the water absorption rate of ceramsite in 1 h, as deduced by an orthogonal test. Xiao et al. [26] investigated the preparation process of the water-treated ceramsite filter material by orthogonal tests with river-dredged sediments as a raw material, indicating that the swelling temperature plays a key role in ceramsite. Currently, most studies use single-factor or orthogonal tests to investigate the influence of the preparation technology on the properties of water-treated ceramsite. These methods are time-consuming and fail to achieve true optimization due to ignoring the interaction between factors. Based on the aforementioned research, the response surface method was used to prepare a sewage-sludge-based composite ceramsite for the first time using the MG removal efficiency as the evaluation factor. The impact factors of the sintering process (sintering time, sintering temperature, and preheating temperature) were considered.

Based on the aforementioned research background, the main objectives of this study are as follows: (1) obtain the sintering parameters of ceramsite with the best adsorption effect on MG by response surface method; (2) to understand the process characteristics of MG adsorption by composite ceramsite; and (3) the adsorption mechanism of MG by composite ceramsite was analyzed. In this study, a sewage-sludge-based ceramsite with a high MG decolorization rate was synthesized for the first time using the response surface method, and the operating parameters in the sintering process were precisely determined. Subsequently, the adsorption characteristics of MG on the ceramsite were verified by adsorption kinetics, isotherms, and thermodynamic modeling. Finally, the adsorption mechanisms were further clarified by FT-IR combined with the 2D-COS analysis method. This study avoids the shortcomings of other methods by using the response surface method to optimize the preparation parameters of ceramsite. Secondly, it provides new insight into designing an effective sludge-based ceramsite for MG adsorption and preliminarily addresses the adsorption mechanism. Finally, it may shed new light on the prospects for expanding the applications of sewage treatment sludge in the ceramsite adsorbent preparation, in addition to finding a possible way to reduce the amount of MG.

2. Materials and Methods

2.1. Raw Materials and Chemicals. The CFA was produced by Dongguan Kewei Environmental Protection Electric Power Company (Dongguan, China). The STS was provided by the Dongguan Sanbird Market sewage treatment station (Dongguan, China), and the moisture content and density of the sludge were 80.21% and 1.132 g/cm^3, respectively. The WG was collected from the City College of the Dongguan University of Technology.

The main composition of the three raw materials was determined by X-ray fluorescence (XRF), and the detailed information is displayed in Table 1. In addition, MG (purity 98%) provided by J&K (Beijing, China) was of the analytical grade. An HCl solution (w/v, 38%) and NaOH (purity 98%) were also of the analytical grade and bought from Tianjin Tianli Chemical Reagent Ltd. (China). Ultrapure water was prepared by the SPI-11-10T apparatus (ULUPURE, Sichuan, China).

2.2. Preparation of Fly Ash/Sludge Composite Ceramic Embryos. Firstly, the STS was air-dried for 24 hours and then placed in a 2 L beaker for standby use. Simultaneously, the WG was simply broken and collected in a 5 L iron container for ball milling (the particle size is less than 20 μm), and the CFA was collected using a 200-mesh sieve (the particle size

Table 1: Composition of three raw materials and as-prepared ceramsite by XRF.

Material type	Weight	Na_2O	MgO	Al_2O_3	SiO_2	K_2O	CaO	Fe_2O_3	P_2O_5	Others
Sludge	(%)	1.084	4.746	32.883	17.994	3.455	11.631	6.237	13.375	8.595
Fly ash		0.767	2.355	29.355	48.193	3.409	8.761	5.64	0.246	1.274
Cullet		10.123	2.342	2.043	77.443	0.353	6.376	0.764	0.101	0.455
Ceramsite		4.605	3.067	19.489	50.833	2.200	8.668	3.869	4.127	3.143

is less than 75 μm). According to the Riley phase diagram, the ceramsite as an adsorption material exhibits the best performance having the chemical composition of SiO_2 (40%~79%), Al_2O_3 (10~25%), and oxide solvent (CaO +MgO+Fe_2O_3+Na_2O+K_2O) (13%~26%). Therefore, this study implemented a variety of mixing ratios. By analyzing the chemical composition under different mixing ratios, the optimal configuration quality ratio was finally determined as 3 (TST): 3 (CFA): 4 (WG). Secondly, TST, CFA, and WG were weighed, respectively, to maintain the quality ratio of the three raw materials at 3 : 3 : 4. Subsequently, these three raw materials were mixed and ground in a ball mill for 20 min (QM-3SP4, Nanjing, China), and then, 30 mL UP-water was injected into the ball milling system. After that, the mixture was taken out for compression molding for 1 h (a DY-10 electrohydraulic prototype). Finally, the sizing mixture was dried at 105°C for 12 h, and then, dried raw pellets (a cylinder with a diameter of 1.0 cm and 0.8 cm in height) were obtained.

2.3. Optimization of the Sintering Conditions of Composite Ceramsite

2.3.1. Influence of a Single Factor on the Adsorption Properties of Ceramsite Investigated by the Control Variable Method. Li et al. [27] reported that the preheating temperature, sintering temperature, and sintering time are the main factors affecting the preparation of ceramsite. Accordingly, by varying these three main factors, numerous ceramic embryos were calcined in an electric muffle furnace (KSL-1200X, Hefei, China), and then, the sintered ceramsite (a cylinder with a diameter of 1 cm and a height of 0.8 cm) was crushed into powder for adsorption experiments. To determine the effect of preheating temperature (300 to 700°C), this study adapted the sintering temperature and sintering time to 1100°C and 15 min, respectively. For the sintering temperature (1000 to 1200°C), the preheating temperature and sintering time were set as 500°C and 15 min, respectively. Similarly, the effect of the sintering time from 5 to 60 min was investigated when the preheating and sintering temperatures were set to 1100 and 500°C, respectively. Finally, a series of composite ceramsite prepared under different operating conditions can be obtained. Subsequently, to evaluate the adsorption properties of as-prepared ceramsite, 0.1 g of the ceramsite samples prepared under different conditions was weighed and then mixed with 30 mL of an MG solution (the initial concentration was 56.876 mg/L). After that, the mixed sample was shaken for 24 h at a shaking speed of 120 rpm. Finally, taking the removal efficiency of MG as an evaluation criterion, the optimal ranges of the preheating temperature, sintering temperature, and sintering time were obtained.

2.3.2. Optimization of the Three Operating Parameters. To further optimize these three operating parameters, the preheating temperature (400, 500, and 600°C), sintering temperature (1050, 1115, and 1180°C), and sintering time (5, 17.5, and 30 min) were taken as the main influencing factors, and each was divided into three levels: low level (-1), medium level (0), and high level (1). According to the different production conditions, 17 adsorbents were prepared. Subsequently, these 17 kinds of as-prepared ceramsite were used to adsorb MG using the same methods described in 2.3.1. Finally, the optimal operating parameters with the best adsorption efficiency on MG were determined. In this paper, the optimal ceramsite composite was named X-Com-ceramsite.

2.4. Evaluation of the Adsorption Properties of the X-Com-Ceramsite. To obtain the adsorption kinetics, 0.1 g of the X-Com-ceramsite and 30 mL of MG testing solution were placed into 50 mL polyethylene vials. The same operation was prepared for 9 sets, and all were performed simultaneously. All the vials were sealed and shaken under 120 rpm and 25°C. Five minutes later, 10 mL of the first samples was withdrawn by a 5 mL pipette from the shaking vials. Subsequently, the corresponding samples were removed from the remaining vials at each sampling time. After filtrating through a 0.45 μm membrane, the samples were analyzed by an ultraviolet spectrophotometer (L5, INESA, Shanghai, China) at a wavelength of 617 nm [28] to determine the MG concentration. All experiments were performed in tripartite, and the mean value was used. For the control, each sorbent was mixed with 0.01 mol/L of $CaCl_2$ solution and operated under identical conditions as mentioned above. To ensure the reliability of experimental results, we used three groups of MG (the initial concentration was 56.876 mg/L). As for adsorption isotherms and thermodynamic modeling, the initial concentration of MG ranged from 27.88 to 139.76 mg/L (isotherm), and the temperature was from 298 to 338 K, respectively. Other operating conditions were the same as those described in the adsorption kinetics except that the sampling time was set as an equilibrium.

To estimate the effects of pH, the testing solution was prepared at several different pH values ranging from 2 to 12, with 0.1 mol/L NaOH or 0.1 mol/L HCl, while the temperature was set to 25°C. The temperature varied from 25 to 65°C, while the pH value was adjusted to 6.0. When temperature and pH were tested as influencing factors,

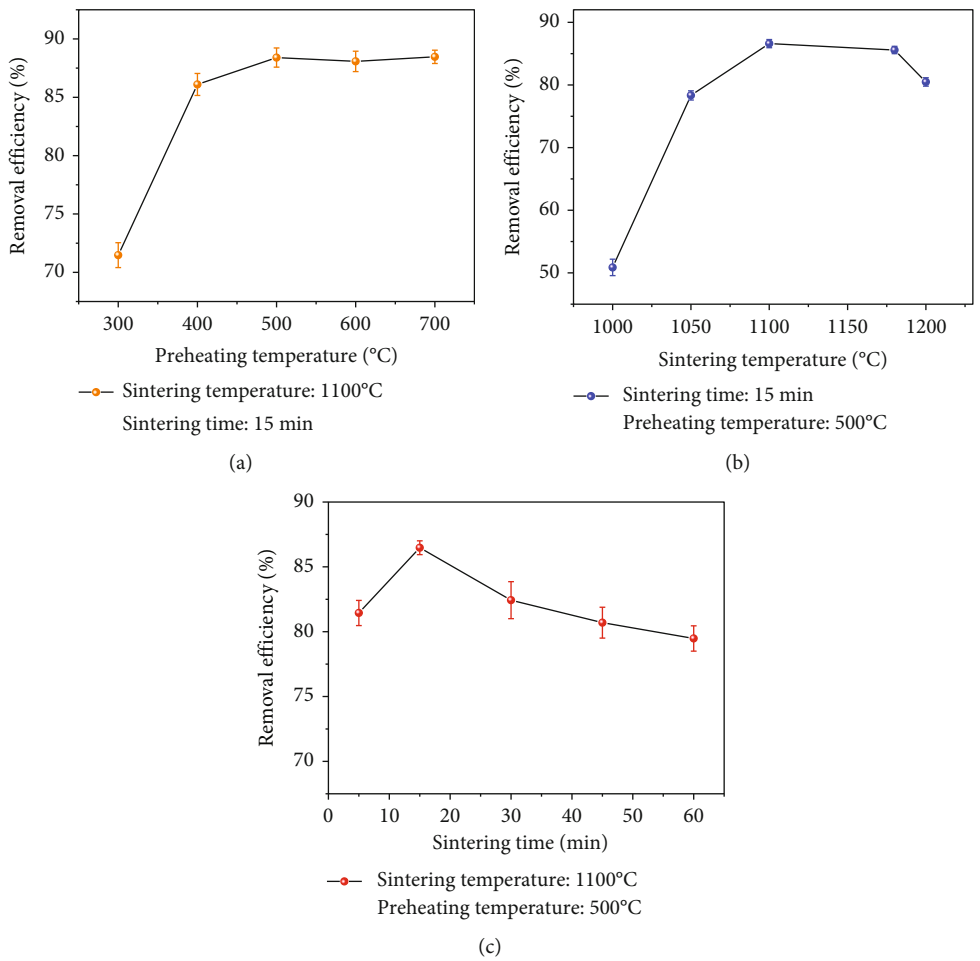

Figure 1: Effects of (a) preheating temperature, (b) sintering temperature, and (c) sintering time on the adsorption of MG on as-prepared X-Com-ceramsite in which the initial concentration of MG was 56.876 mg/L and the adsorption time was set to 24 h.

the initial concentration of MG was 86.406 and 56.876 mg/L, respectively.

2.5. Analysis. The detailed surface morphology and microstructure of the as-prepared X-Com-ceramsite were examined by using the SEM (JSM-6360LV, China). The FT-IR (FT-IR-650; Guangdong, China) were measured using 32 scans with a 4 cm^{-1} resolution to measure the functional groups on the surface of samples. Furthermore, the FT-IR spectra were analyzed by 2D-COS to study the sorption mechanism of MG on the surface of the X-Com-ceramsite. 2D Shige software (Kwansei Gakuin University, Japan) was used to transform the data into a new spectral matrix for generating 2D-COS synchronous and asynchronous correlation spectroscopy maps. X-ray fluorescence (XRF) analysis was used to determine the phase composition of the powder composite ceramsite. The zeta potential of the ceramsite was monitored by a zeta potential analyzer (Malvern Zetasizer Nano S90, England). The ceramsite was ground to powder and then immersed in NaCl solution (1 mmol/L) to form a mixture (0.1 g/L). NaOH or HCl was used to adjust the pH value of the mixture (2.0-12.0). After 30 min of ultrasonic treatment (25°C, 40 kHz), the mixture was aged for 24 h, and then, the zeta potential was measured. The residual concentrations of MG were measured by an ultraviolet spectrophotometer (L5, INESA, Shanghai, China), in which the maximum absorption wavelength can be decided at 617 nm, respectively. The mass of MG adsorbed on the X-Com-ceramsite (q_t) and the sorption efficiency (W) of MG were given by the following equations:

$$q_t = \frac{C_0 - C_t}{M} \times V, \tag{1}$$

$$W = \frac{C_0 - C_t}{C_0} \times 100\%, \tag{2}$$

where C_0 represents the initial concentration of MG (mg/L) and C_t is the residual concentration of sorbate at time t (mg/L). V and M are the volume of solution (L) and the mass of the X-Com-ceramsite (g), respectively.

3. Results and Discussion

3.1. Optimization of the Preparation Conditions for Composite Ceramsite. The single-factor experiments show that the suitable ranges of preheating temperature, sintering temperature,

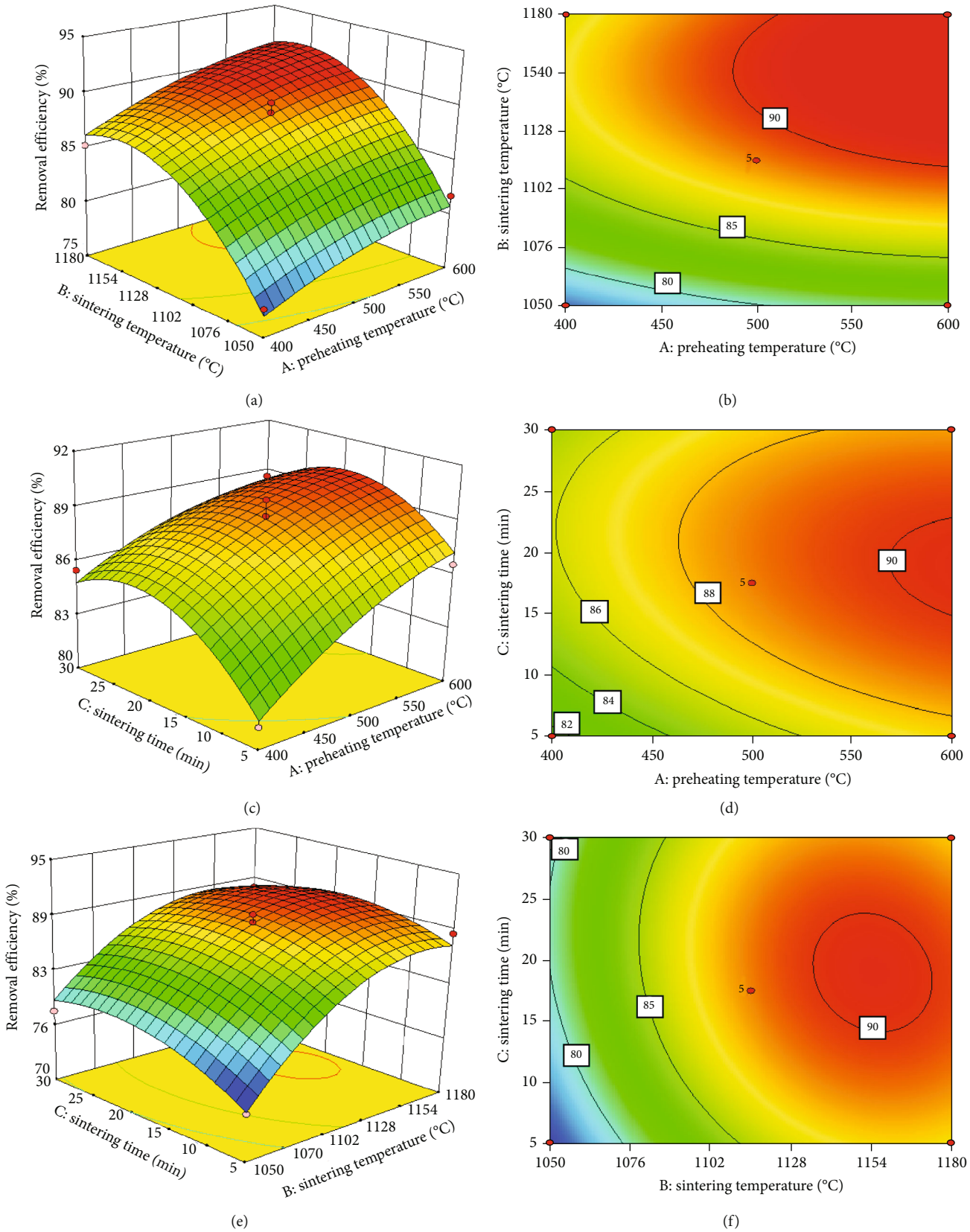

Figure 2: (a) Response surface plot and (b) contour line map decolorization efficiency of MG sintering temperature vs. preheating temperature. (c) Response surface plot and (d) contour line map decolorization efficiency of MG sintering time vs. preheating temperature. (e) Response surface plot and (f) contour line map decolorization efficiency of MG sintering temperature vs. sintering time (the initial concentration of MG was 56.876 mg/L and the adsorption time was set to 24 h).

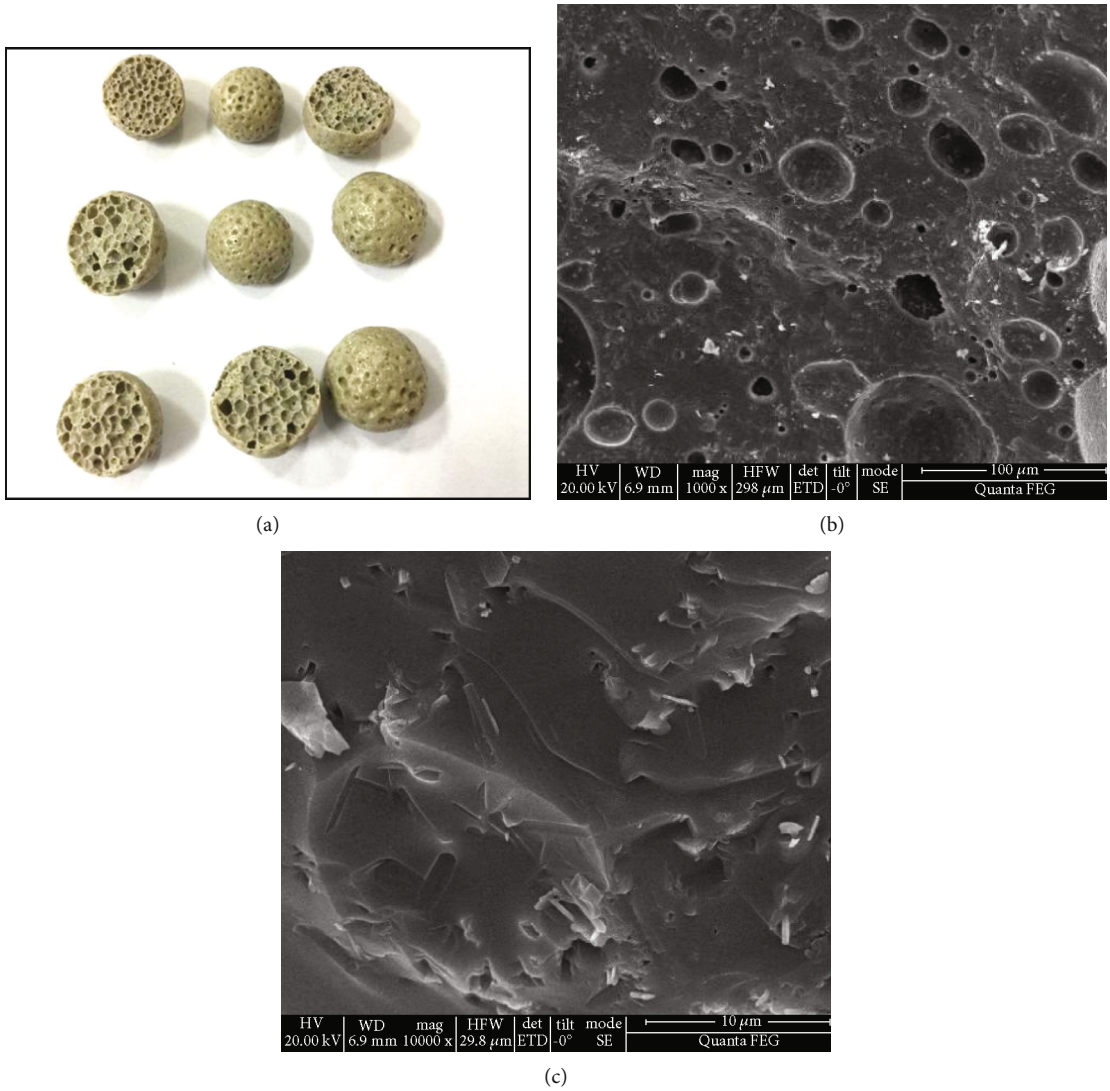

(a) (b) (c)

Figure 3: (a) The outlook of as-prepared X-Com-ceramsite. (b) SEM image of X-Com-ceramsite (low magnification). (c) SEM of the sample at higher magnification.

and sintering time are 400~600°C, 1050~1180°C, and 5 min~30 min, respectively (Figure 1). The values of three operational parameters and one response for all 17 runs by the Box-Behnken design are shown in Table S1. The regression analysis of the response surface was carried out by a data processing program built into the software, and the results are shown in Table S2. Finally, the quadratic polynomial equation of the factor was obtained. This equation includes a set of coefficients and coded factors described as follows: $Y = 88.78 + 2.30A + 4.98B + 1.10C + 0.27AB - 0.95AC - 0.88BC - 0.86A^2 - 4.04B^2 - 2.04C^2$.

Variables A, B, and C are preheating temperature, sintering temperature, and sintering time, respectively; Y represents the removal efficiency of MG.

As shown in Table S2, the F-value, P value, and SNR of the model are 32.54, <0.0001, and 85.34, respectively, implying that the model is significant and relevant. The determination coefficient R^2 is 0.9767, and the variation coefficient C.V.% is 1.30 < 10%, which indicates that the model fits the actual situation with high reliability and precision. Therefore, the model can well reflect the effect of the operating conditions of ceramsite preparation on the removal efficiency of MG. According to the results of the F-value, the effect relationship of each factor is as follows: sintering temperature (161.84) > preheating temperature (34.48) > sintering time (7.82). In addition, according to the significance of the quadratic regression model (P value), the interaction between B and C is significant ($P < 0.1$ for BC), indicating that the sintering temperature and the sintering time have strong effects.

Figure 2 shows that the removal rate of MG among all factors shows an elliptic trend, and the corresponding two-dimensional contour curve exhibits a considerable curvature in the contour curve, indicating that these three factors are interdependent, showing a significant interaction. As shown in Figures 2(b) and 2(c), when the sintering time and sintering temperature remain unchanged, the higher the preheating temperature, the higher the removal

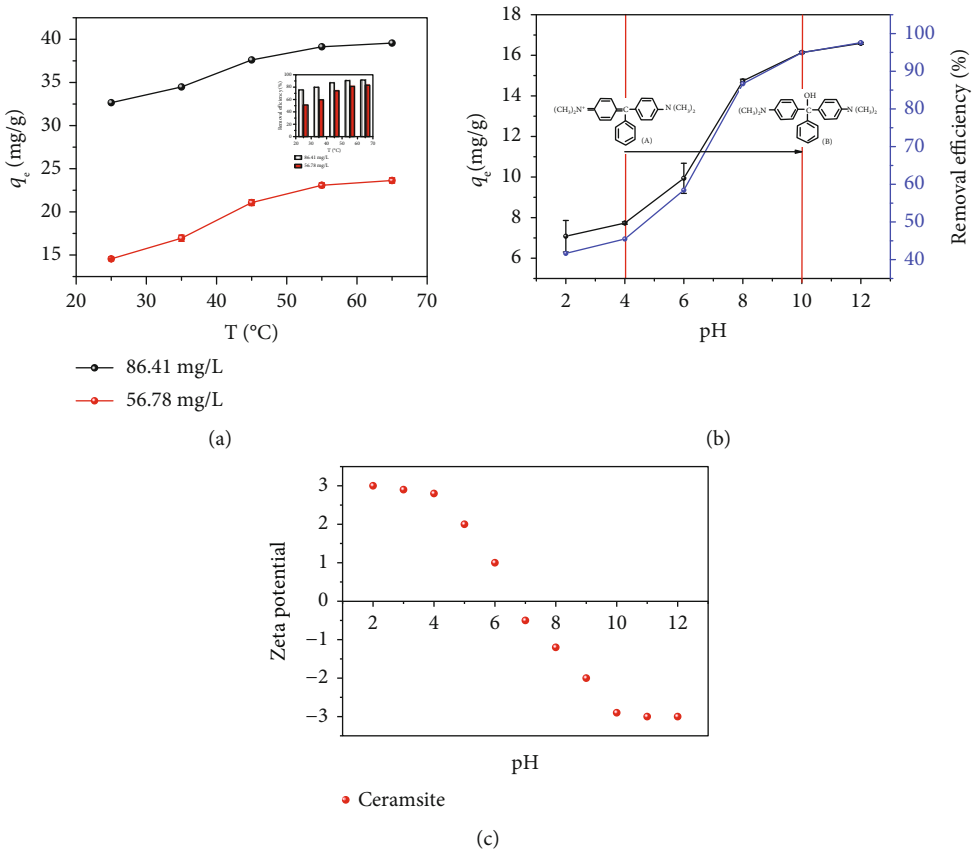

Figure 4: (a) Effects of temperature on the adsorption of MG by the X-Com-ceramsite in which the value of pH is 6.8. (b) Effects of pH on the adsorption of MG by the X-Com-ceramsite (the value of T was set to 25°C). (c) Zeta potential of the ceramsite.

rate of MG. Li et al. [27] found that gas production increases with the preheating temperature (10 min), which further leads to the development of pores in the ceramsite. Therefore, the developed pores in the ceramsite can act as adsorption sites for MG removal, subsequently increasing the removal efficiency, which is in perfect agreement with the phenomenon observed above. Unlike the preheating temperature, the removal rate first increases with the sintering temperature and then slightly decreases (Figures 2(b) and 2(d)). Wu et al. [29] reported that as the sintering temperature rises, the melting rate of glass melts increases, which, on the one hand, brings about the expansion of the ceramsite and, on the other hand, can also enhance gas release, forming connecting holes. Consequently, the removal efficiency is further improved by the increased number of adsorption sites. However, when the firing temperature reaches a level too high for the material, it leads to a partial closure of external connecting holes. Meanwhile, dense and small pores inside the blank can be slowly ablated into larger pores, which decreases the removal rate. For the sintering time, as shown in Figures 2(c) and 2(d), when the preheating temperature and the firing temperature remain unchanged, the removal rate of MG shows a similar trend as in the case of sintering temperature (first increases and then decreases) with the change in the sintering time. Ren [30] explained that the liquid phase in a billet increases gradually with the sintering time. As liquid and gas phases gradually reach an equilibrium, the ceramsite expands due to the developed pore structure, and the interlocking pores gradually form. As a result, there is an improvement in the removal efficiency because of the increased number of adsorption points. However, when the firing time exceeds about 18 min, the excess liquid phase in the billet causes the honeycomb-like pore to change into a macroporous pore structure. In particular, the liquid phase can jam the inner bore and interconnected pores, so the removal rate of MG decreases.

Finally, through the regression equation analysis, the optimal process conditions for the preparation of ceramsite are as follows: preheating temperature, sintering temperature, and sintering time are 600°C, 1157°C, and 17 min, respectively. Three parallel experiments were carried out using the above preparation conditions, and the results showed that the relative errors between the measured values and the predicted values were less than 4%. Therefore, it can be confirmed that the prediction performance of this model is reliable, and it can reflect the influence of various ceramsite preparation factors on the removal rate of MG.

3.2. Characteristics of the X-Com-Ceramsite. As shown in Table 1, the main components of the raw materials for the sludge composite ceramsite include Na_2O, MgO, Al_2O_3, SiO_2, K_2O, CaO, Fe_2O_3, and P_2O_5. Among them, SiO_2 accounts for almost half of the mass of the as-prepared

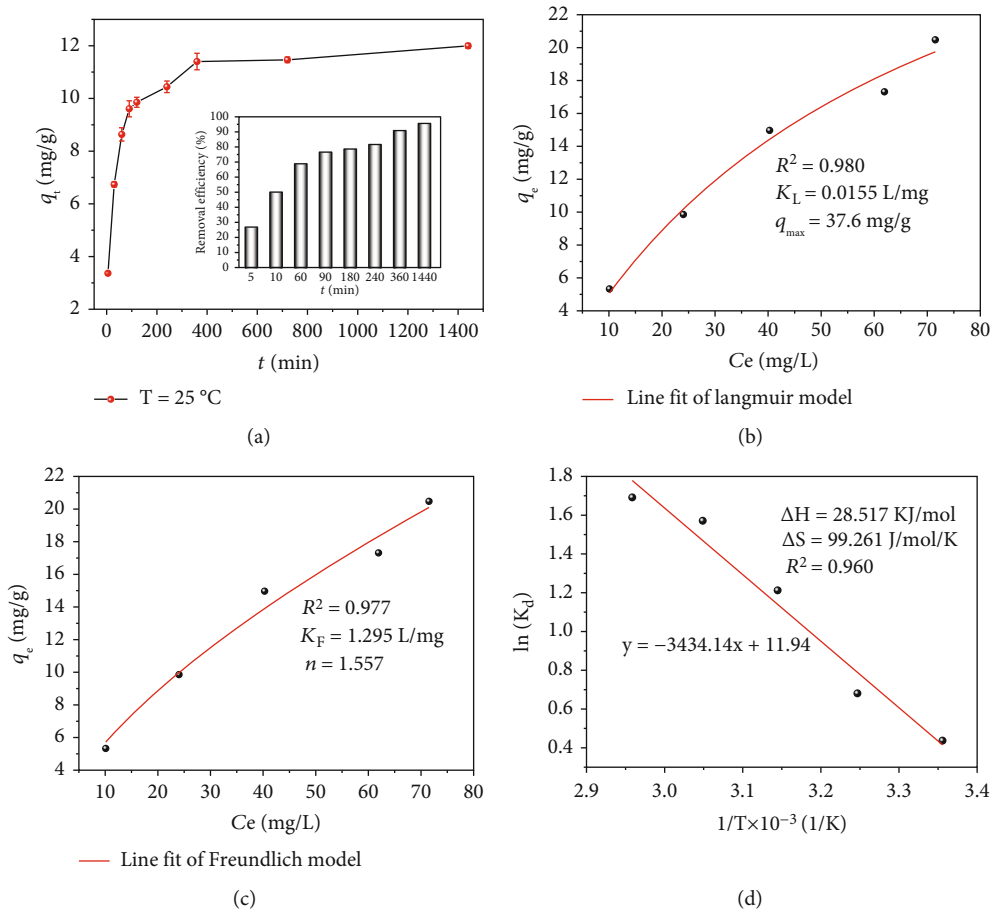

Figure 5: (a) Effect of contact time on the sorption of MG by the X-Com-ceramsite in which the initial concentration of MG was 56.876 mg/L (insert is the removal efficiency of MG under different contact time). (b) Langmuir model, (c) Freundlich model, and (d) Van't Hoff equation fitting the adsorption of MG on the X-Com-ceramsite.

composite ceramsite, followed by Al_2O_3, which takes up 20%. The physical diagram (Figure 3(a)) shows that the ceramsite prepared in this study presents a cylindrical shape. Moreover, the pore structure of the cut samples is very well-developed. This pore structure can act as a channel for pollutants to reach the interior and exterior surfaces of the adsorbent. The SEM images show that the exterior surface of the X-Com-ceramsite sample exhibits rough features and a various number of different-sized apertures formed during the sintering process (Figure 3(b)). Evidently, as discussed before, sintering of materials at high temperatures breaks down the organic-rich sludge to produce CO_2, and when the carbon dioxide escapes, tiny pores are left behind. As can be seen from Figure 3(c), the internal surface of the composite ceramsite is rough, and acicular or lamellar crystal bundles and staggered arrangement can be observed on the surface, indicating that the internal specific surface area of the composite ceramsite is considerably large.

3.3. Adsorption of MG on the X-Com-Ceramsite

3.3.1. Effects of Temperature and pH on the Adsorption Process. As shown in Figure 4(a), when the temperature increased from 25 to 55°C, the q_e value of MG (the initial concentrations were 56.876 and 86.406 mg/L) shows an increasing trend, and the decolorization rate of MG increases rapidly (from 20% to 90%). However, when the temperature exceeds 55°C, there are no significant changes in the decolorization rate of MG, indicating that, before reaching 55°C, the elevated temperature is beneficial to the adsorption of MG on the X-Com-ceramsite. As Figure 4(b) shows, the adsorption amount for MG exhibits an upward trend with the pH value. Since the value of pHpzc for the as-prepared ceramsite is 6.7 (Figure 4(c)), it is positively or negatively charged at pH 2.0 or 12.0. At low pH, MG mainly exists in the form of MG^+ (the pKa is 6.9) [31]. Therefore, the repulsion between MG and the X-Com-ceramsite surface leads to a relatively low adsorption effect. In contrast, when increasing the pH value, the number of positive charges on the surface of the ceramsite decreases, and they are replaced by negative charges, while MG molecules are electroneutral at a high pH value. As a result, a lesser repulsive force between MG and the surface of the ceramsite significantly increases adsorption efficiency.

3.3.2. Adsorption Kinetics. As shown in Figure 5(a), during the initial stage, the adsorption amount (q_t) increases rapidly from 0 to 9.52 mg/g because of the fast transfer of MG to the

Table 2: Parameters of the kinetic models for the adsorption of MG by X-Com-ceramsite.

Model	Parameter	X-Com-ceramsite
Pseudo-first-order		
	$q_{e,\exp}$ (mg/g)	11.99
	$q_{e,\mathrm{cal}}$ (mg/g)	5.207
	K_1 (h^{-1})	0.005
	R^2	0.982
Pseudo-second-order		
	K_2 (g/(mg·h))	0.003
	$q_{e,\mathrm{cal}}$ (mg/g)	12.169
	R^2	0.999
	$K_2 q^2_{e,\mathrm{cal}}$ (mg/(h·g))	0.480
Weber and Morris intraparticle diffusion		
	K_{id1} (mg/g·$h^{1/2}$)	0.968
	I_1 (mg/g)	1.234
	R^2	0.988
	K_{id2} (mg/g·$h^{1/2}$)	0.173
	I_2 (mg/g)	7.927
	R^2	0.936
	K_{id3} (mg/g·$h^{1/2}$)	0.042
	I_3 (mg/g)	10.37
	R^2	0.906

surface of the adsorbent particles. From 100 to 400 min, the q_t value shows a slowly increasing trend (9.52 to 11.34 mg/g) and then an almost unchanged trend (11.34 to 11.99 mg/g) from 400 to 1440 min. The pseudo-first-order kinetic model, the pseudo-second-order kinetic model, and the Weber and Morris internal particle diffusion were used to clarify the adsorption kinetics of MG on the X-Com-ceramsite in the overall adsorption.

All the parameters for the three models are listed in Table 2. The pseudo-second-order kinetic model shows a better fit of the R^2 value of 0.999, suggesting that the whole adsorption process is a chemisorption process. That means that the adsorption between MG and adsorbent occurs through orbital valency by sharing or exchanging electrons. Furthermore, the calculated q_e values are much closer to the actual experimental data (11.99 mg/g) than the one calculated from the pseudo-first-order equation. Furthermore, it can be found that all the values of I are not equal to 0, suggesting that the rate-controlling step for the adsorption of MG on the adsorbents proceeds simultaneously by the boundary layer and intraparticle diffusion rather than through one of them alone. The diffusion coefficient of K_{id1} (0.968 mg/g.$\mathrm{min}^{1/2}$) is higher than that for both K_{id2} (0.173 mg/g.$\mathrm{min}^{1/2}$) and K_{id3} (0.042 mg/g.$\mathrm{min}^{1/2}$), indicating the fast mass transfer rate of MG from the aqueous liquid to X-Com-ceramsite particles. The I values are arranged in the order of $I_1 < I_2 < I_3$, indicating that the boundary layer effect of MG on the X-Com-ceramsite is the most significant [32].

3.3.3. Adsorption Isotherm and Thermodynamic Modeling. Two isotherm models and one thermodynamic model (Freundlich, Langmuir, and the Van't Hoff equation) were employed:

$$q_e = K_F C_e^{1/n}, \tag{3}$$

$$q_e = \frac{q_m K_L C_e}{1 + K_L C_e}, \tag{4}$$

$$\ln k_d = -\frac{\Delta G}{RT} = -\frac{\Delta H}{RT} + \frac{\Delta S}{R}, \tag{5}$$

where C_e is the residual concentration of sorbate in an equilibrium (mg/L), q_e is the uptake of sorbate per unit mass of sorbent (mg/g); K_F (mg/$L^{(1-1/n)}$·g) and n are the Freundlich constants, represent the adsorption capacity and intensity, respectively; q_m is the maximum sorption amount (mg/g), and K_L is Langmuir constant (L/mg); Kd is the thermodynamic equilibrium constant; ΔG represents the Gibbs free energy (kJ/mol); k_d is the thermodynamic equilibrium constant; R is the molar gas constant (8.314 J/(mol·K)); T is the thermodynamic temperature (K); ΔH and ΔS represent Enthalpy Changes (kJ/mol) and Entropy changes (J/(mol·K)), respectively.

Figures 5(b)–5(d) show the fitting results of all the data. The Langmuir isotherm model has a better fit with R^2 = 0.980 (Figure 5(b)), indicating that the adsorption is a monolayer coverage process. Based on the $q_{\max}$ values, it can be concluded that the maximum potential adsorption capacity of the MG toward the X-Com-ceramsite is 37.6 mg/g. The Freundlich constant n ($1 < n < 10$) demonstrates that the adsorption of MG on the X-Com-ceramsite is favorable.

According to Figure 5(d) and Table 3, the adsorption free energy ΔG is less than 0 in the whole temperature range, and the value of ΔG decreases with the temperature, indicating that the adsorption process of MG on the composite ceramsite is spontaneous. However, the values of ΔH and ΔS for the whole adsorption process are greater than 0, suggesting that the MG adsorption process on the X-Com-ceramsite is endothermic and the degree of disorder enhances in the whole adsorption process. It can be concluded that the as-prepared ceramsite has a good adsorption affinity for MG.

3.4. Adsorption Mechanism Analysis. The infrared spectra of MG at different concentrations adsorbed by the X-Com-ceramsite are shown in Figure 6(a). The bottom line shows the information on the X-Com-ceramsite functional groups. The middle and top lines represent the light energy group information of the X-Com-ceramsite after adsorbing 20 to 50 mg/L of MG. The peak at 3422 cm^{-1} is attributed to the stretching vibration of crystal water [33]. The peaks at 2922 and 2852 cm^{-1} are assigned to the C-H stretching vibration of $-CH_3$ and $-R_2CH_2$ groups, representing aliphatic methylene groups assigned to fats and lipids [34]. The peak at 1619 cm^{-1} is attributed to the symmetric vibration of carboxylate [34]. The band near 1384 cm^{-1} is related to the

Table 3: Parameters of the thermodynamic model describing the adsorption of MG.

Temperature (K)	Parameters					
	Q_e (mg/g)	C_e (mg/L)	K_d	ΔG (KJ/mol)	ΔS (J/mol.K)	ΔH (KJ/mol)
298	32.656	21.093	1.083	-1.548		
308	34.476	17.454	1.743	-1.975		
318	37.608	11.189	3.205	-3.361	28.550	99.261
328	39.137	8.131	4.285	-4.813		
338	39.558	7.288	4.753	-5.428		

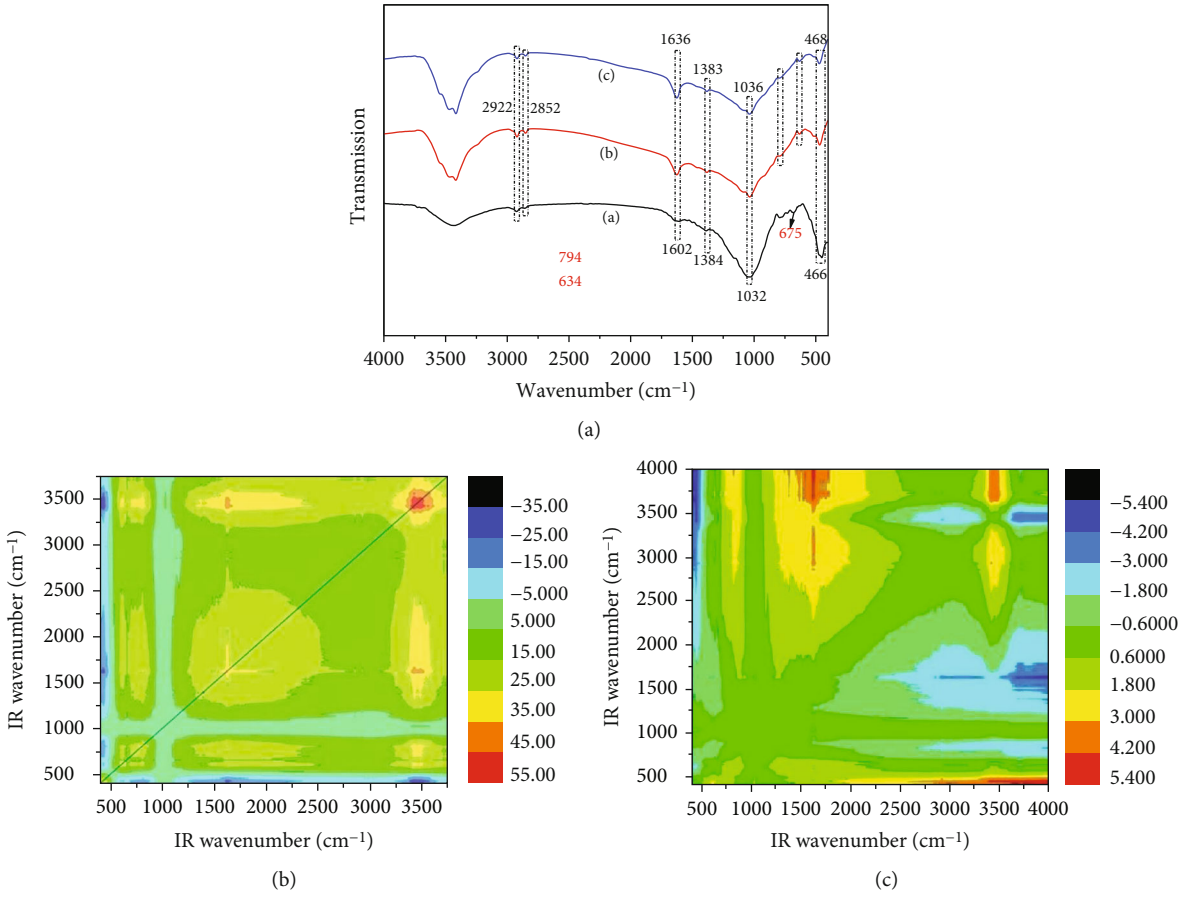

Figure 6: (a) FT-IR spectra of X-Com-ceramsite and X-Com-ceramsite after adsorbed different concentrations of MG. (b) Synchronous 2D correlation maps and (c) asynchronous 2D correlation maps generated from the Fourier transform FT-IR map.

Table 4: The assignment of absorption bands in FT-IR spectra and signs of each cross peak in the synchronous (Φ) and asynchronous (Ψ) maps.

Position (cm^{-1})	Assignment	Sign					
		3422	2922	1619	1384	1032	669
3422	ν_{O-H} (crystal water)	+	+(-)	+(+)	+(+)	+(-)	+(-)
2922/2852	ν_{C-H} (-CH_3/-R_2 CH_2)		+	+(+)	+(+)	+(-)	+(+)
1619	ν_{COO-} (carboxylate)			+	+(+)	+(-)	+(+)
1384	δ_{C-H} (aliphatics)				+	+(-)	+(-)
1032	ν_{C-O-O} or ν_{C-O} (carbohydrates)					+	+(+)
669	CO_3^{2-}						+

Signs were obtained in the maps of 2D-COS map: + positive and - negative.

absorption of C-H deformation vibrations in methyl groups [35]. A sharp band at about 1032 cm^{-1} is mainly attributed to C-O-O and C-O, indicating carbohydrate occurrence [20]. The band at 669 cm^{-1} is due to CO_3^{2-} [33]. As shown in Figure 6(a), it is found that the peaks of the original ceramsite at 3422, 1602, and 1032 cm^{-1} are shifted to 3416, 1619, and 1032 cm^{-1} after adsorption. Moreover, the peak at 669 cm^{-1} disappears after the MG adsorption, and two new peaks appear at 794 and 634 cm^{-1}. The results indicate that almost all the groups appearing in the infrared spectrum are involved in the adsorption of MG. The 2D-COS was further used to analyze the FT-IR data to sequence the binding affinity of the functional groups carried by the X-Com-ceramsite toward MG. The data of 2D-COS analysis of FT-IR are shown in Figures 6(b) and 6(c) by using software 2D Shige. On the diagonals of the synchronization graph (Figure 6(b)), there are six self-intersecting positive peaks and one negative peak appeared at the main diagonal, and seven cross-peaks are observed on both sides of the diagonal, indicating that the signal of the functional groups on the surface of the X-Com-ceramsite also changes as the MG concentrations change. In the asynchronous map (Figure 6(c)), seven cross peaks located at 3422/2922 cm^{-1}, 3422/1032 cm^{-1}, 3422/669 cm^{-1}, 2922/1032 cm^{-1}, 1602/1032, 1384/1032 cm^{-1}, and 1384/669 cm^{-1} are negative, and eight positive peaks are located at 3422/1619 cm^{-1}, 3422/1384 cm^{-1}, 2922/1619, 2922/1384, 2922/669, 1619/1384 cm^{-1}, 1619/669, and 1032/669 cm^{-1}. The signs of each cross peak in the synchronous (Φ) and asynchronous (Ψ) maps are listed in Table 4. According to Noda's rule, when the wavelength $\lambda_1 > \lambda_2$, (1) if $\Psi(\lambda_1, \lambda_2)$ in the asynchronous correlation diagram is positive and the associated synchronous correlation peak $\Phi(\lambda_1, \lambda_2)$ is also positive, indicating that the change of spectral intensity preferentially occurs at high wavenumber λ_1, and if the associated synchronous correlation peak $\Phi(\lambda_1, \lambda_2)$ is negative, the change in spectral intensity preferentially occurs at low wavenumber λ_2. (2) If $\Psi(\lambda_1, \lambda_2)$ is also negative and the associated synchronous correlation peak $\Phi(\lambda_1, \lambda_2)$ is positive, it means that the spectral intensity change occurs preferentially at the low wavenumber λ_2, and if the related synchronous correlation peak $\Phi(\lambda_1, \lambda_2)$ is negative, it means that the spectral intensity change occurs preferentially at the high wavenumber λ_1. Thus, it can be concluded that the sequence of the binding affinities of MG follows such order: C-O/C-O-O (1032 cm^{-1}) > -R_2CH_2 (2922 cm^{-1}) > O-H (3422 cm^{-1}) > -COO(1619 cm^{-1}) > CO_3^{2-} (669 cm^{-1}) > C-H (1384 cm^{-1}), which means that the C-O/C-O-O functional group carried by the carbohydrates is the most sensitive to the changes in the initial concentration of MG.

4. Conclusion

In this paper, a composite ceramsite adsorbent was prepared for the decolorization of MG using CFA and STS as the main materials and WG as a functional additive. The optimum parameters in sintering process are obtained (the preheating temperature, sintering temperature, and sintering time are 600°C, 1157°C, and 17 min, respectively). The pseudo-second-order kinetic model presented a good fit, indicating a chemisorption process, i.e., valency force through sharing or exchange of electrons between MG and X-Com-ceramsite. The maximum adsorption amount (q_m) was calculated to be 37.6 mg/g on the basis of the Langmuir model. It was found that the adsorption capacity of MG could be improved by increasing the temperature or pH value of adsorption system appropriately. The functional groups (crystal water, carboxylate, aliphatics, etc.) carried by X-Com-ceramsite were proved to be the adsorption sites for extracting MG from aqueous solution. The binding affinity of these groups toward MG was sequenced as -C-O/C-O-O (1032 cm^{-1}) > -R_2CH_2 (2922 cm^{-1}) > O-H (3422 cm^{-1}) > -COO (1619 cm^{-1}) > CO_3^{2-} (669 cm^{-1}) > C-H (1384 cm^{-1}), suggesting that the carbohydrate group played a significant role in the adsorption of MG.

Data Availability

All data, models, or code that support the findings of this study are available from the corresponding author upon reasonable request.

Conflicts of Interest

The authors declare that they have no known competing financial interests or personal relationships that could have appeared to influence the work reported in this paper.

Authors' Contributions

Weicheng Fang was responsible for the data curation and writing the original manuscript, reviewing, and editing. Xingxing Cheng was assigned for writing the original manuscript and visualization. Chang-Jung Sun was tasked for the formal analysis. Hongfei Xiao was charged for writing the original manuscript. Jing Wang was responsible for the conceptualization and funding acquisition.

Acknowledgments

This work was financially supported by the Social Technology Development Project of Dongguan City in China (No. 2020507151153), the University-Level Major Research and Cultivation projects of Dongguan City College (2020YZD001Z), and the Guangdong University Teaching Quality and Teaching Reform Project (Experimental Teaching Demonstration Center No. 30). The author would like to thank the Instrument Analysis Center of Dongguan City College for technical support.

Supplementary Materials

The analysis principle of software 2D Shige for 2D-COS has been added in text S1, and the kinetic equations and all the defined symbols were added in the Supplementary Materials text S2. The values of three operational parameters and one response for all 17 runs by the Box-Behnken design are shown in Table S1. The regression analysis of the response surface was carried out by a data processing program built

into the software, and the results are shown in Table S1. *(Supplementary Materials)*

References

[1] M. Roosta, M. Ghaedi, and A. Asfaram, "Simultaneous ultrasonic-assisted removal of malachite green and safranin o by copper nanowires loaded on activated carbon: central composite design optimization," *RSC Advances*, vol. 5, no. 70, pp. 57021–57029, 2015.

[2] A. Ahmad, S. H. Mohd-Setapar, C. S. Chuong et al., "Recent advances in new generation dye removal technologies: novel search for approaches to reprocess wastewater," *RSC Advances*, vol. 5, no. 39, pp. 30801–30818, 2015.

[3] W. Jie, G. Y. Hou, L. K. Wu, H. Z. Cao, G. Q. Zheng, and Y. P. Tang, "A novel adsorbent of three-dimensional ordered macro/mesoporous carbon for removal of malachite green dye," *Journal of Central South University*, vol. 27, no. 2, pp. 388–402, 2020.

[4] A. Dabrowski, "Adsorption — from theory to practice," *Advances in Colloid and Interface Science*, vol. 93, no. 1-3, pp. 135–224, 2001.

[5] L. Jiang, J. Y. Zhan, X. M. Li, J. Luo, Q. Yang, and Y. Wang, "Adsorption of phosphate from wastewater by fly ash ceramsite," *Acta Scientiae Circumstantiae*, vol. 31, no. 7, pp. 1413–1420, 2011.

[6] Q. Shao, H. Xu, M. M. Tong, and S. Li, "The technical study on the preparation of lightweight ceramsite made from sewage sludge and fly ash," *Advanced Materials Research*, vol. 356-360, pp. 1871–1875, 2012.

[7] X. Y. Luo, W. F. Li, and X. L. Jin, "Effect of aggregate size and gradation on the ceramsite sound-absorbing materials," *Advanced Materials Research*, vol. 216, pp. 450–457, 2011.

[8] Z. G. Guo, M. L. Ma, and B. Liu, "The research progress on sludge treatment and disposal technology," *Journal of Hebei GEO University*, vol. 42, no. 1, pp. P59–P63, 2019.

[9] C. B. Wu, Y. F. Yang, S. X. Zhu, X. L. Ren, and F. T. Zhao, "Grey relational analysis between particle size distribution of power storage porous ceramsite and thermal conductivity of PCM gypsum board," *Advanced Materials Research*, vol. 158, pp. 130–139, 2011.

[10] B. C. Fu and C. S. Dai, "Study on preparation of functional ceramsite (GTL) from paper sludge and its adsorption properties for Cu^{2+}," *Advances in Environmental Protection*, vol. 10, no. 3, pp. 332–341, 2020.

[11] W. H. Zhu, T. Yu, Z. P. Guo, D. Y. Wei, T. He, and H. J. Zhang, "Phosphorus removal performance of novel ceramsite made from water treatment sludge and fly ash," *Chinese Journal of Environmental Engineering*, vol. 12, no. 10, pp. 2741–2750, 2018.

[12] M. Wu, L. Y. Zhao, and X. Feng, "Efficiency and influence factors of arsenic removal by constructed wetland substrates," *Journal of Yangtze River Scientific Research Institute*, vol. 32, no. 6, pp. 42–48, 2015.

[13] Q. Zhang, J. Hu, D. J. Lee, Y. Chang, and Y. J. Lee, "Sludge treatment: current research trends," *Bioresource Technology*, vol. 243, pp. 1159–1172, 2017.

[14] Y. L. Wei, S. H. Cheng, K. T. Ou, P. J. Kuo, T. H. Chung, and X. Q. Xie, "Effect of calcium compounds on lightweight aggregates prepared by firing a mixture of coal fly ash and waste glass," *Ceramics International*, vol. 43, no. 17, pp. 15573–15579, 2017.

[15] G. Yang, G. Zhang, and H. Wang, "Current state of sludge production, management, treatment and disposal in China," *Water Research*, vol. 78, pp. 60–73, 2015.

[16] B. Dong, X. Liu, L. Dai, and X. Dai, "Changes of heavy metal speciation during high-solid anaerobic digestion of sewage sludge," *Bioresource Technology*, vol. 131, pp. 152–158, 2013.

[17] M. S. Shehu, Z. A. Manan, and S. R. W. Alwi, "Optimization of thermo-alkaline disintegration of sewage sludge for enhanced biogas yield," *Bioresource Technology*, vol. 114, no. 114, pp. 69–74, 2012.

[18] M. K. Jamali, T. G. Kazi, M. B. Arain, H. I. Af Ridi, N. Jalbani, and A. R. Memon, "Heavy metals from soil and domestic sewage sludge and their transfer to sorghum plants," *Environmental Chemistry Letters*, vol. 5, no. 4, pp. 209–218, 2007.

[19] X. Zhao, H. Zhao, X. Huang, L. Wang, and P. Ji, "Effect and mechanisms of synthesis conditions on the cadmium adsorption capacity of modified fly ash," *Ecotoxicology and Environmental Safety*, vol. 223, no. 1, article 112550, 2021.

[20] X. Song, Z. Cui, M. Xing, and Y. D. Li, "Effect of fly ash and slag on mechanical properties of cement soil under dry-wet cycles," *Ningxia Engineering Technology*, vol. 21, no. 1, pp. 40–43, 2022.

[21] X. Zhu, Q. Zhang, W. Zhang, J. Shao, and X. Wu, "Experimental study on the basic properties of a green new coal mine grouting reinforcement material," *ACS Omega*, vol. 5, no. 27, pp. 16722–16732, 2020.

[22] Y. Feng, Y. Zhang, X. Quan, and S. Chen, "Enhanced anaerobic digestion of waste activated sludge digestion by the addition of zero valent iron," *Water Research*, vol. 52, pp. 242–250, 2014.

[23] Q. Wan, Q. J. Han, and X. Zhang, "Preparation and performance optimization of ceramsite using waste sludge," *Journal of the Chinese Ceramic Society*, vol. 38, no. 4, pp. 1228–1236, 2019.

[24] H. X. Cheng, H. Zhou, and J. H. Li, "Experimental study on manufacturing haydite by sintering municipal sludge and its incineration ash," *Chinese Journal of Environmental Engineering*, vol. 10, no. 2, pp. 845–850, 2016.

[25] H. Rong, H. F. Zhang, and L. Zhang, "Optimization of sludge ceramsite baking system and its effect on ceramsite performance," *New Building Materials*, vol. 46, no. 4, pp. 68–87, 2019.

[26] J. Xiao, Z. Huang, Y. Chen, Q. U. Qian, and S. Chu, "Preparation and properties analysis of sediment ceramsite with high efficiency phosphorus removal," *Journal of Zhejiang University of Agriculture and Forestry*, vol. 36, no. 2, pp. 415–421, 2019.

[27] T. P. Li, T. Sun, and D. Li, "Preparation, sintering behavior, and expansion performance of ceramsite filter media from dewatered sewage sludge, coal fly ash, and river sediment," *Journal of Material Cycles & Waste Management*, vol. 20, pp. 71–79, 2016.

[28] M. Shirmardi, A. H. Mahvi, B. Hashemzadeh, A. Naeimabadi, G. Hassani, and M. V. Niri, "The adsorption of malachite green (MG) as a cationic dye onto functionalized multi walled carbon nanotubes," *The Korean journal of chemical engineering*, vol. 30, no. 8, pp. 1603–1608, 2013.

[29] J. N. Wu, X. L. Zhou, B. Yang, W. Y. Shi, and Y. Wu, "Lytag preparation and study on its treatment for simulated printing and dyeing wastewater," *Industrial Safety and Environmental Protection*, vol. 8, pp. 73–76, 2014.

[30] X. Ren, *Preparation of Adsorbent from Water Treatment Plant Wastewater Sludge and the Removal Efficiency for Hexavalent*

Chromium, [Ph.D. thesis], Harbin Institute of Technology, 2014.

[31] I. Šafařík and M. Šafaříková, "Detection of low concentrations of malachite green and crystal violet in water," *Water Research*, vol. 36, pp. 196–200, 2008.

[32] F. C. Wu, R. L. Tseng, and R. S. Juang, "Initial behavior of intraparticle diffusion model used in the description of adsorption kinetics," *Chemical Engineering Journal*, vol. 153, no. 1-3, pp. 1–8, 2009.

[33] M. Grube, J. G. L. Lin, P. H. Ee, and S. Kokorevicha, "Evaluation of sewage sludge-based compost by FT-IR spectroscopy," *Geoderma*, vol. 130, no. 3-4, pp. 324–333, 2006.

[34] L. L. Bai, Z. C. Zheng, C. L. Wang, C. H. Wang, X. Liu, and H. L. Jiang, "Multi-spectroscopic investigation on the complexation of tetracycline with dissolved organic matter derived from algae and macrophyte," *Chemosphere*, vol. 187, pp. 421–429, 2017.

[35] Y. Fan, C. Zheng, A. Huo et al., "Investigating the binding properties between antimony(V) and dissolved organic matter (DOM) under different pH conditions during the soil sorption process using fluorescence and FTIR spectroscopy," *Ecotoxicology and Environmental Safety*, vol. 181, pp. 34–42, 2019.